Study of Various C-Shaped Armatures in Electromagnetic Launcher

M. Sajjad Bayati and Kambiz Amiri

Department of Electrical Engineering
Razi University, Kermanshah, Iran
s.bayati@razi.ac.ir

Abstract ─ The current density distribution on the cross section of the rails is affected by the geometry and dimensions of the rails and armature. This paper analyzed a rectangular railgun that is formed by two parallel rails and an armature with various geometries. Rail thickness (w_r), width (h_r), and separation (s_r) between two rails are equal to 2 cm, 4 cm and 4 cm, respectively. C-shaped armatures have three corners that are named front, back and arm side of armature which rounded step by step. All case studies simulated with the Finite Element Method Three Dimensions (FEM3D). For all steps, the inductance gradient, normal force, current density (J) distribution and maximum values of J are computed. The force between rails and armature named normal force. This force and pressure can be changed the rails and armature form. Friction force is increasing with increasing normal force. Maximum current densities occur at the armature corners and contact section between the rails and armature. These phenomena can produce a hot point that fuse the railgun and must be considered in armature and rail designing. This paper investigates the effect of armature geometry and dimensions on current density distribution, maximum value of current density, inductance gradient and normal force or normal pressure on armature.

Index Terms ─ Current density, FEM, inductance gradient, normal force, railgun.

I. INTRODUCTION

Armature and rails are the two main components of a railgun that are usually made up of materials with higher electrical conductivity. In a simple railgun, the magnetic flux density is generated around rails by passing electric current through them. Magnetic force has two components (normal and axial) which are exerted on armature due to magnetic flux density and the current passed through the armature. The axial force (F_x) is proportional to the inductance gradient (L') and passing current (I) through the rails [1-4]:

$$F_x = \frac{1}{2} L' I^2. \tag{1}$$

The distribution of electric current density over the armature is very high at the contact edges between the armature and rails, and sharp corners of the armature. These points become very hot due to Ohmic losses, hence deformed and after each launch reduce working life of the rails [5-8]. In recent years, significant advances researches have been reported for the railgun. Armature geometry can be assumed simple shape such as cube C and U-shape [9-15]. Passing currents through the up and bottom of the C-shape cause repulsive force between them. This force causes enormous pressure on the inner cross section of rails. This pressure can lead to rail breakage or rail bending too.

To reduce the losses and normal force on armature (contact with rails), we can reduce the amplitude of the input current. But reducing the amplitude of applied current will be decreased the force on the armature.

In Fig. 1 shows a railgun with C-shape armature in 3D and side view of 2D. The objective of this work is to analyze the C-shape armature with and without any rounded in the front, throat and rear side. These structures are simulated with FEM and calculated the inductance gradient, J_{max}, and normal force. These quantities are dependent on various sizes of armature and rounded radiuses. We presented the optimize dimensions for minimum value of the J_{max} and maximum value of the inductance gradient.
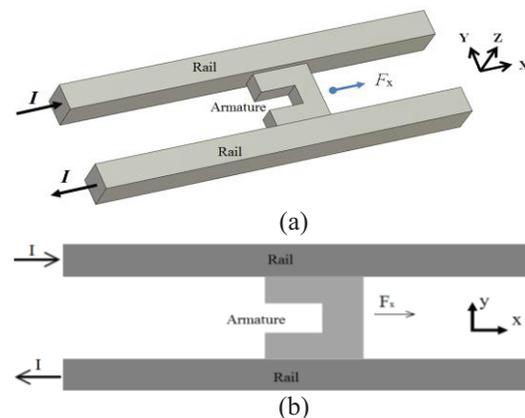

Fig. 1. Structure of railgun: (a) 3D railgun and (b) side view.

II. PROBLEM STATEMENT

A railgun consist of two parallel rails and a solid armature. Rails and armature are formed a closed current loop. Both rails made of copper and connected to an electrical power supply, and solid armature made of aluminum. The dimensions of the copper rails are as follows; width (h_r), separation (s_r) and thickness (w_r) are 4, 4, and 2 cm, respectively.

A. Railgun structure and parameters

Figure 2 (a) shows the rear view of railgun. The width of armature (h_a) is less than or equal rail's width.

Figure 2 (b) displays the side view of C-shape armature with details of dimensions and applied force.

According to Fig. 2 (b), we design three curvatures at the front, rear and throat of the C-shape armature with R_1, R_2 and R_3 radius, respectively.

In this paper, first C-shape armature without any rounded (Fig. 1), second C-shape armature with rounded in the front, throat and rear side are simulated and analyzed. Inductance gradient, J_{max}, and normal force are calculated for various sizes of X_C, Y_C, R_1, R_2 and R_3. Optimized results according to minimum value of the J_{max} and maximum value of the inductance gradient for various geometries and sizes are presented in the two different tables.

B. Force diagram

The electromagnetic force (F) on the armature is depicted in Fig. 3. For the calculation of the electromagnetic force with ANSYS, we assume that the injected current has a constant amplitude.

We used FEM to compute the magnetic force for two and three-dimensional. For 2D, we first calculated the magnetic energy (E_m) than,

$$F = \nabla E_m; \qquad (2)$$

and for 3-D simulation,

$$\vec{F} = \int \vec{J} \times \vec{B} \, dv , \qquad (3)$$

where J and B are current density and magnetic flux density, respectively.
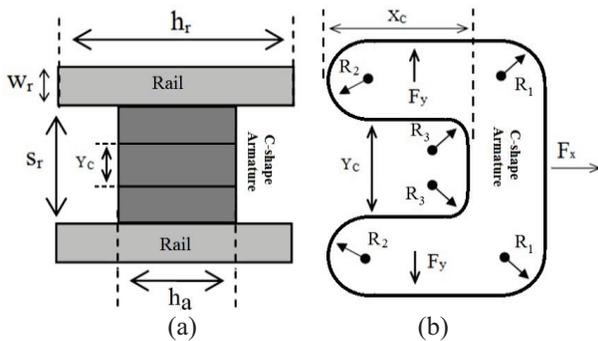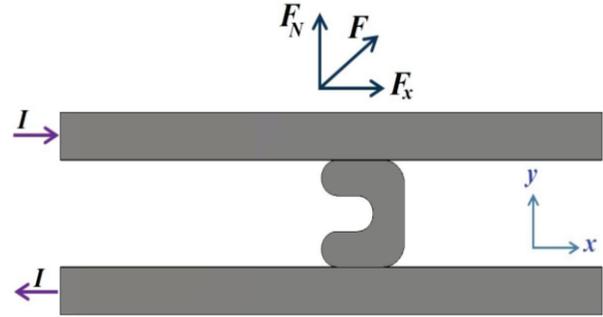

Fig. 3. The electromagnetic force and components.

F has two components, axial force (F_x) and normal force (F_y). The axial force (F_x) is propulsion force that can move the armature along the rails that is shown in Figs. 1-3. The friction force is a function of the normal force that is exerted by the normal force (F_y) and the friction coefficient.

C. Boundary conditions and modeling

Both rails are connected to electrical power supply and the total current flow is the same in two rails, but opposite directions that is displayed in Fig. 1. According to the Fig. 4 (a), the structure is symmetric to x-z and x-y plans, and only the first quadrant shown in Fig. 4 (b) is modeled.

The x-y plan (in 2D view y axis) is a symmetrical boundary and replaced by "magnetic wall" or H_t=0, and the x-z plan (in 2D view z-axis) is an asymmetrical boundary and can be replaced by "electrical wall" or H_n=0. We proposed the three models for 3D simulation of the railgun: 1) a half of the rails and armature by using magnetic wall, 2) one rail and a half of the armature by using electric wall, 3) a half of a rail and a quarter of the armature, that are shown in Figs. 5 (a), (b) and (c), respectively. Finally, this paper modeled only the quadrant of total structure (see Fig. 5 (c)). The symmetrical and asymmetrical boundaries are replaced by magnetic and electrical walls, respectively.

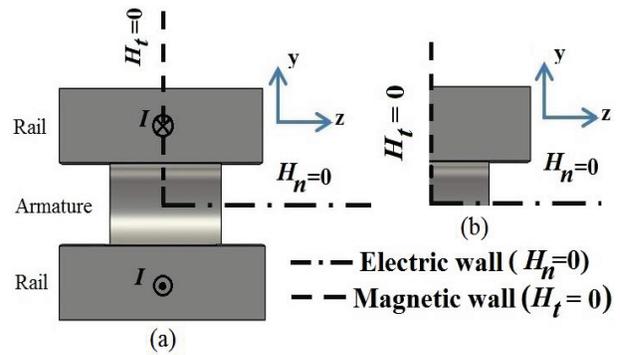Fig. 2. (a) Rear view of railgun, and (b) side view of C-shape armature.

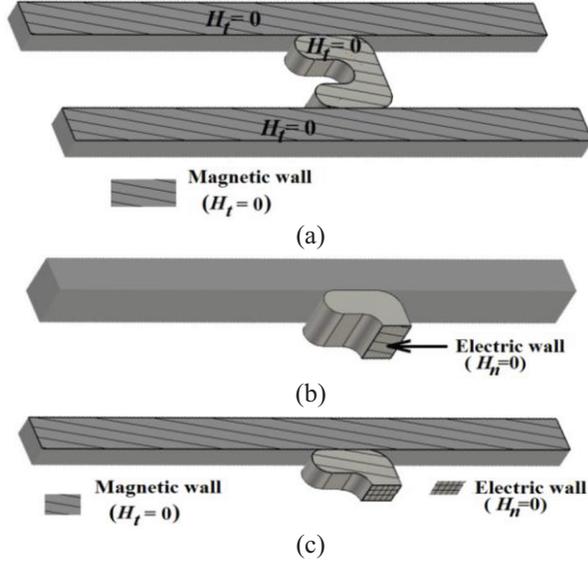Fig. 4. Boundary conditions in rear view of railgun with C-shape armature.

Fig. 5. 3D railgun: (a) half magnetic wall, (b) half electric wall, and (c) a quadrant of 3D railgun using magnetic and electric walls.

III. NUMERICAL RESULTS

In this section, inductance gradient, distribution of the current density and normal force are calculated for with and without rounded in each corner. The optimum structures with different size are obtained by considering two factor maximum value of inductance gradient and minimum value of J_{max}.

A. Inductance gradient and normal force

Table 1 shows the L', J_{max} and F_y for $h_a=h_r=4$ cm and different values of X_C and Y_C without rounded all the corners [5]. According to this table, the inductance gradient show minor variations of approximately 2%. The normal force variations show an increase of size more than 2.5 times for different values.

For the maximum current density by the way, a maximum increase less than 20% is observed. h_a is reduced to 1.6 cm, and L' obtained 0.5374 and 0.5238 µH/m for $X_C=Y_C=2$ cm and $X_C=Y_C=3$ cm, respectively.

L' and F_y are computed for C-shape armature with rounded front side and shown in Table 2. Rounded radius (R_1) equals to 0.50, 1.00, 1.50 and 1.90 cm. This Table illustrated that F_y decreased slightly with increasing R_1. The L' increased with increasing R_1. The rate of variations for L' for $X_C=Y_C=3$ cm is larger than other sizes. L' and F_y are calculated for C-shape armature with rounded front and arm side and shown in Table 3. Rounded radius for arm side (R_2) equals to 0.30, 0.36, 0.40 and 0.50 cm. Finally, back side is rounded with R_3 radius. R_3 equals to 0.45, 0.90 and 1.35 cm. Table 4 shows L' and F_y for different sizes of all dimensions. According to this table, L' and F_y are increased with

increasing R_3. h_a is reduced to 2 cm, and L' obtained 0.5571 µH/m for $X_C=Y_C=2$ cm, $R_1=1.8$ cm, $R_2=0.44$ cm, $R_3=1.35$cm, which is larger than 0.49467 µH/m for $h_a=4$ cm. For $X_C=Y_C=3$ cm, $R_1=1.8$ cm, $R_2=0.2$ cm, $R_3=1.35$ cm, L' is 0.5963 µH/m, which is larger than and 0.54771 µH/m.

Table 1: The inductance gradient, maximum current density and normal force applied to the C-shape armature without rounded for different value of X_C and Y_C

X_C (cm)	Y_C (cm)	L' (µH/m)	J_{max} (10^{12}A/m^2)	F_y (kN)
1		0.4804	1.31	132
2	1	0.4843	1.39	254
3		0.4844	1.55	380
1		0.4812	1.32	131
2	2	0.4852	1.39	241
3		0.4832	1.53	349
1		0.4804	1.26	115
2	3	0.4823	1.27	197
3		0.4772	1.47	276

Table 2: The inductance gradient and normal force applied to the C-shape armature with rounded at front side

R_1 (cm)	$X_C=Y_C=1$ cm		$X_C=Y_C=2$ cm		$X_C=Y_C=3$ cm	
	F_y (kN)	L' (µH/m)	F_y (kN)	L' (µH/m)	F_y (kN)	L' (µH/m)
0.50	129	0.4808	237	0.4870	271	0.4812
1.00	125	0.4817	232	0.4885	268	0.4881
1.50	121	0.4832	226	0.4919	271	0.4969
1.90	117	0.4861	222	0.4962	274	0.5061

Table 3: The inductance gradient and normal force applied to the C-shape armature with rounded at front and arm side

X_C (cm)	Y_C (cm)	R_1 (cm)	R_2 (cm)	F_y (kN)	L' (µH/m)
2.40	2.40	1.60	0.36	225	0.4952
2.40	2.00	1.60	0.30	254	0.4961
2.40	1.80	1.00	0.50	234	0.4876
2.00	2.00	1.00	0.40	197	0.4867
1.60	2.00	1.00	0.30	164	0.4850

Table 4: The inductance gradient and normal force applied to the C-shape armature with rounded at front, back and arm side

R_3	$X_C=Y_C=2$ cm, $R_1=1.8$ cm, $R_2=0.44$ cm		$X_C=Y_C=3$ cm, $R_1=1.8$ cm, $R_2=0.2$ cm	
	F_y (kN)	L' (µH/m)	F_y (kN)	L' (µH/m)
0.45	183	0.49037	263	0.5003
0.90	184	0.49102	267	0.5349
1.35	185	0.49467	274	0.5477

B. Optimization according to L' and maximum value of current density

We want to reduce the maximum value of current density and increase inductance gradient. For both conditions two tables are presented. Table 5 shows the optimum structures according to inductance gradient. The maximum value of L' is 0.53555 µH/m for the C-shape armature without rounded corners. When all corners are rounded, L' increasing to 0.54771 and 0.59625 µH/m for h_a equals to 4 and 2 cm, respectively.

Table 6 shows the minimum value of J_{max}. According to this table, minimum value of J_{max} is 1.09×10^{12} A/m² for rounded all three corners.

Table 5: Optimization according to maximum value of the inductance gradient for various geometries (Units: L' (µH/m) and J_{max} (10^{12}A/m²))

X_C	Y_C	R_1	R_2	R_3	h_a	J_{max}	L'
3	3	1.8	0.44	1.35	2	4.30	0.5962
3	3	1.8	0.44	1.35	4	1.97	0.5477
2.4	2	1.6	0.3	-	4	1.40	0.4961
3	3	1.9	-	-	4	1.39	0.5061
2	2	-	-	-	1.6	2.16	0.5356

Table 6: Optimization according to minimum value of the maximum current density for various geometries (Unit: cm)

X_C	Y_C	R_1	R_2	R_3	h_a	J_{max} (10^{12}A/m²)	L' (µH/m)
2	2	1.8	0.2	1.35	4	1.09	0.49088
2	2	1.00	0.4	-	4	1.22	0.48674
3	3	0.5	-	-	4	1.25	0.48126
2	2	-	-	-	4	1.39	0.48526
1	3	-	-	-	4	1.26	0.48040

C. Current and normal force distribution on the armature

Due to the skin effect, the current tends to flow on the outer surface on the armature. Figure 6 shows the current density distribution on the quadrant of C-shape armature for $X_C=Y_C=3$ cm with rounded in all corners. For $h_a=4$ and 2 cm, these distributions are shown in Figs. 6 (a) and (b), respectively. Velocity skin effect can be by higher current density concentrations at the outer edge of rear armature surface.

With compared between Figs. 6 (a) and (b), can be said the J_{max} increased with decreasing h_a. Figure 7 shows the normal force distribution on the quadrant of C-shape armature for $X_C=Y_C=3$ cm with rounded in all corners. For $h_a=4$ and 2 cm, these distributions are shown in Figs. 7 (a) and (b), respectively.

Figure 8 shows the current density distribution on the quadrant of C-shape armature for $X_C=Y_C=2$ cm with rounded in all corners. For $h_a=4$ and 2 cm, these distributions are shown in Figs. 8 (a) and (b), respectively.

According to this figure, the J_{max} occurs in two places. That is located at the junction of rails and front and back side of armature. The J_{max} at the arm side in Fig. 8 increased than in Fig. 6. With compared between Figs. 8 (a) and (b), can be said the current density is increased with decreasing h_a. Figure 9 shows the normal force distribution on the quadrant of C-shape armature for $X_C=Y_C=2$ cm with rounded in all corners. For $h_a=4$ and 2 cm, these distributions are shown in Figs. 9 (a) and (b), respectively.
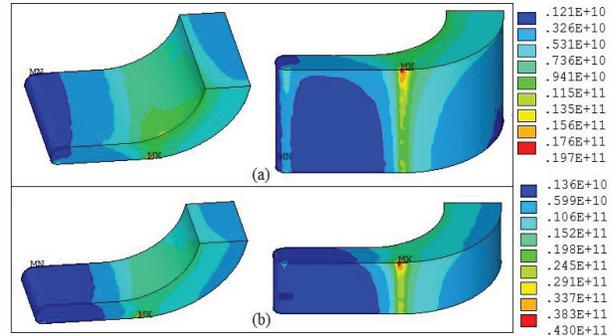

Fig. 6. Current density distribution on the C-shape armature for $X_C=Y_C=3$ cm: (a) $h_a=4$ cm and (b) $h_a=2$ cm.
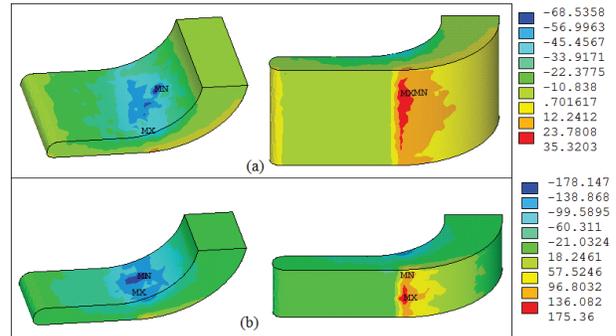

Fig. 7. Normal force distribution on the C-shape armature for $X_C=Y_C=3$ cm: (a) $h_a=4$ cm and (b) $h_a=2$ cm.
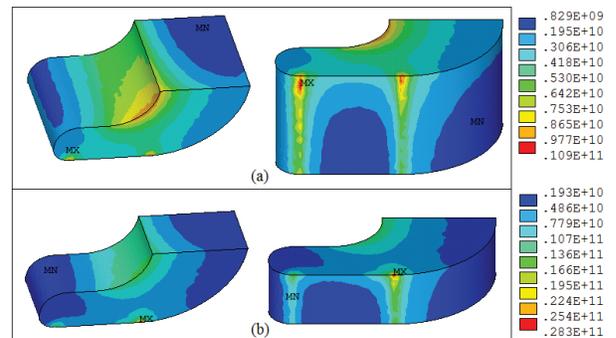

Fig. 8. Current density distribution on the C-shape armature for $X_C=Y_C=2$ cm: (a) $h_a=4$ cm and (b) $h_a=2$ cm.
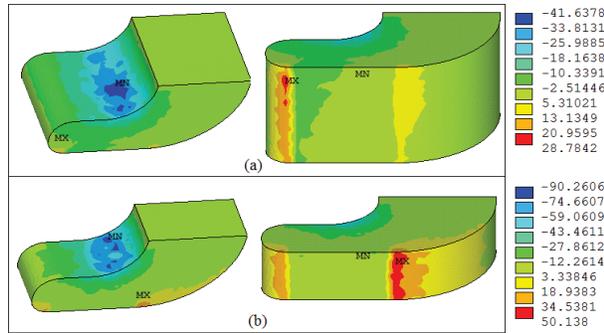
Fig. 9. Normal force distribution on the C-shape armature for $X_C=Y_C=2$ cm: (a) $h_a=4$ cm and (b) $h_a=2$ cm.

IV. CONCLUSION

This paper investigated the effect of C-shape armature geometry on the inductance gradient, normal force and the maximum electrical current density. According to the results of this paper can be said, increasing X_C results in the slightly variations of L', increase the J_{max} and F_y. Increasing Y_C results in the slightly variations of L' and J_{max} and decrease the F_y. Variations of the all rounded radius result in slightly on the normal force. Increasing the X_C and Y_C result in the effect of R_1, R_2 and R_3 on L' and J_{max} and F_y will be more.

REFERENCES

[1]   M. S. Bayati, A. Keshtkar, and A. Keshtkar, "Transition study of current distribution and maximum current density in railgun by 3D FEM and IEM," *IEEE Transactions on Plasma Science*, vol. 39, no. 1, pp. 13-17, Jan. 2011.

[2]   R. A. Marshall, "Railgun bore geometry round or square?," *IEEE Transactions on Magnetics*, vol. 35, no. 1, pp. 427-431, Jan. 1999.

[3]   A. Keshtkar, S. Bayati, and A. Keshtkar, "Derivation of a formula for inductance gradient using IEM," *IEEE Transactions on Magnetics*, vol. 45, no. 1, pp. 305-308, Jan. 2009.

[4]   M. S. Bayati and A. Keshtkar, "Study of the current distribution, magnetic field, and L' of rectangular and circular railguns," *IEEE Transactions on Plasma Science*, vol. 45, no. 5, pp. 1376-1381, May 2013.

[5]   L. Chen, J. He, Z. Xiao, and Y. Pan, "Three-dimensional numerical simulation of the joule heating of various shapes of armatures in railguns," *IEEE Transactions on Plasma Science*, vol. 39, no. 1, pp. 456-460, Jan. 2011.

[6]   J. F. Kerrisk, "Electrical and thermal modelling of railgun," *IEEE Transactions on Magnetics*, vol. MAG-20, no. 1, pp. 339-402, 1984.

[7]   H. Vanicek and S. Satapathy, "Thermal characteristics of a laboratory electromagnetic launcher," *IEEE Transactions on Magnetics*, vol. 41, no. 1, pp. 188-193, Jan. 2005.

[8]   J. D. Powell and A. E. Zielinski, "Ohmic heating in a double-taper sabot-armature," *IEEE Transactions on Magnetics*, vol. 39, no. 1, pp. 153-157, Jan. 2003.

[9]   L. Rip, S. Satapathy, and K-T. Hsieh, "Effect of geometry change on the current density distribution in C-shaped armature," *IEEE Transactions on Magnetics*, vol. 39, no. 1, pp. 72-75, Jan. 2003.

[10] M. S. Bayati, "Projectile geometry," 16th *EML Symposium*, China, June 2012.

[11] B-K. Kim and K-T. Hsieh, "Effect of rail/armature geometry on current density distribution and L'," *IEEE Transactions on Magnetics*, vol. 35, no. 1, pp. 413-416, Jan. 1999.

[12] L. Chen, J. He, Z. Xiao, and Y. Pan, "Augmentation of current ramp-down contact pressure in C-shaped armature railguns," *IEEE Transactions on Plasma Science*, vol. 39, no. 1, pp. 48-52, Jan. 2011.

[13] D. C. Haugh and G. M. G. Hainsworth, "Why "C" armature work (and why they don't!)," *IEEE Transactions on Magnetics*, vol. 39, no. 1, pp. 52-55, Jan. 2003.

[14] S. Xia, J. He, L. Chen, Z. Xiao, and J. Li, "Studies on interference fit between armatures and rails in railguns," *IEEE Transactions on Plasma Science*, vol. 39, no. 1, pp. 186-191, Jan. 2011.

[15] Q. Lv, Z. Li, B. Lei, K. Zhao, Q. Zhang, H. Xiang, and S. Xie, "Primary structural design and optimal armature simulation for a practical electromagnetic launcher," *IEEE Transactions on Plasma Science*, vol. 45, no. 5, pp. 1403-1409, May 2013.

Mohammad Sajjad Bayati was born in Sonqor, Kermanshah, Iran, in 1979. He received the B.Sc. degree in Electrical Engineering from the University of Tabriz, in 2002, the M.Sc. in Telecommunication Field and Wave Engineering from the Sahand University of Technology, and the Ph.D. degree in Electrical Engineering from the University of Tabriz in 2011. His M.Sc. dissertation was focused on DF antenna and Ph.D. dissertation was focused on analysis of rail electromagnetic launcher

using combined FEM-3D and IEM in time domain.

He is an Assistant Professor with the Department of Electrical Engineering, University of Razi, Kermanshah, Iran. His research interests include electromagnetic, mathematical in electromagnetic, electromagnetic launcher, bio and microstrip antenna.

Kambiz Amiri was born in Kermanshah, Iran, 1981. He received the B.Sc. degree in Electrical Engineering in 2008. He is currently working toward the M.Sc. degree in the Department of Electrical Engineering, Razi University, Kermanshah. His research interests include electromagnetic and antenna design.